Journal of Molecular Structure 1199 (2020) 127037

Contents lists available at ScienceDirect

Journal of Molecular Structure

journal homepage: http://www.elsevier.com/locate/molstruc

Novel cyanoacetamide integrated phenothiazines: Synthesis, characterization, computational studies and *in vitro* antioxidant and anticancer evaluations

Kannan Gokula Krishnan [a], Chandran Udhaya Kumar [a], Wei-Meng Lim [b], Chun-Wai Mai [b, c], Punniyakoti V. Thanikachalam [b], Chennan Ramalingan [a, *]

[a] Department of Chemistry, School of Advanced Sciences, Kalasalingam Academy of Research and Education (Deemed to be University), Krishnankoil, 626 126, Tamilnadu, India
[b] School of Pharmacy, International Medical University, 126 Jalan Jalil Perkasa 19, 57000, Bukit Jalil, Kuala Lumpur, Malaysia
[c] Center for Cancer and Stem Cell Research, Institute for Research, Development and Innovation (IRDI), International Medical University, 126, Jalan Jalil Perkasa 19, 57000, Bukit Jalil, Kuala Lumpur, Malaysia

ARTICLE INFO

Article history:
Received 28 April 2019
Received in revised form
25 August 2019
Accepted 4 September 2019
Available online xxx

Keywords:
Anticancer
Antioxidant
Computation
Cyanoacetamide
Phenothiazine

ABSTRACT

A series of novel phenothiazine based cyanoacrylamides **6a-d** have been synthesized from phenothiazine through multistep synthetic strategy. The structure of these novel molecules (**6a-d**) has been determined by FT-IR, ^{1}H NMR and ^{13}C NMR spectral techniques. Computational studies were carried out for the synthesized compounds **6a-d** using DFT method with B3LYP/6-311G(d,p) basis set. The target compounds **6a-d** have been screened for their *in vitro* antioxidant and anticancer activity. The antioxidant data revealed that the compounds **6c** and **6d** exhibited high radical scavenging activity with IC_{50} value of 37.32 and 39.07 μM, respectively. Furthermore, all the synthesized compounds displayed significant *in-vitro* anticancer activity against both the pancreatic tumor cells AsPC1 and SW1990. Particularly, the compound **6c** exhibited the highest activity among the molecules tested against both the tumor cells *viz*., AsPC1 and SW1990.

1. Introduction

Cancer is a leading cause of death around the globe, which claims over six million people died a year and still increasing (WHO) [1]. Nearly two hundred types of cancers have been identified, which affects the major parts of organs [2]. Although various drugs have been developed, discovery of new drugs to combat specific cancers is highly essential. On the other hand, to enhance the anticancer properties of the existing molecules, various synthetic approaches have been established on the basis of structural modifications [3]. Generally, molecules having heteroatoms are considered as structural motifs for drug development as they increases the host-guest connectivity between the molecule and the biological receptors through hydrogen bonding [4,5]. The bi- and tri-cyclic heterocycles *viz*. indole, imidazoles, thiazoles, quinolones, acridine, carbazole, phenothiazine, are significant platforms for a wide range of drugs which can offer new prospects for controlled manipulation of genome [6]. Among these heterocycles, phenothiazine ring systems as one of the most abundant ones and becoming precious molecular scaffold in medicinal, industrial and academic fields. Chlorpromazine, a derivative of phenothiazine has been used to treat psychotic disorders and allergy [7]. Thioridazine, trifluoperazine, promethazine and azaphenothiazines are some of the phenothiazine analogues showed very promising clinical trials for the treatment of patients with different cancers [8]. Further, remarkable growth has been documented on the synthesis and applications of these derivatives owing to their medicinal and next-generation applications [9–18].

On the other hand, nitrile and amide possessing chemical entities are the versatile lead molecules with many potential bioactivities attributed to pharmacological applications [19]. A large number of nitrile and amide systems are found in many natural products [20]. They have been widely used in initial pre-clinical trials as anti-fungal [21], anti-oxidant [22], anti-viral [23] and anti-cancer agents [24]. These structural cores with the

* Corresponding author.
E-mail addresses: ramalinganc@gmail.com, c.ramalingan@klu.ac.in (C. Ramalingan).

https://doi.org/10.1016/j.molstruc.2019.127037
0022-2860/

encouraging biological activities inspired us to prosecute the investigation with these molecular analogues. Hence, we designed phenothiazine based cyanoacetamides as a new class of antioxidant and anticancer agents. The synthesis of new series of compounds has been achieved by employing multistep synthetic protocol and physical, spectroscopic and structural studies have also been carried out. Antioxidant and anticancer activities of the synthesized molecules have been evaluated using DPPH method and cell viability assay method, respectively.

2. Experimental

2.1. General

The melting points reported herein were measured in open-capillaries and are uncorrected. Progress and completion of the reactions were monitored by TLC on pre-coated Silica gel 60 F plates using hexane and ethyl acetate as eluents. FT-IR spectra of the synthesized molecules were recorded as KBr pellet form with number of scans equals 16 using Shimadzu-IR Tracer 100 in the range of 400–4000 cm^{-1}. The spectral features are reported in wavenumber (cm^{-1}). ^{1}H and ^{13}C NMR spectra were recorded at 400 MHz and 100 MHz, respectively on a Bruker spectrometer using deuterated chloroform and deuterated dimethyl sulfoxide as solvents. Chemical shift values are reported in parts per million (ppm) from tetramethylsilane (TMS), an internal standard. ^{1}H NMR splitting patterns are designated as singlet (s), broad singlet (br s), doublet (d), doublet of doublet (dd) and multiplet (m).

2.2. Synthesis

The synthetic intermediates, alkylphenothiazines **3a-c** and phenothiazine carbaldehydes **4a-d** were synthesized using literature methods [18].

2.3. Synthesis of phenothiazenyl cyanoacrylamide *6a*

To a solution of phenothiazine carbaldehyde **4a** (0.5 g, 0.2 mmol) in acetonitrile, were added cyanoacetamide (0.17 g, 0.2 mmol) and catalytic amount of piperidine. The reaction mixture was refluxed for 4 h and the reaction progress was monitored by TLC. After cooling, the reaction mixture was poured into water and extracted with dichloromethane. The combined organic layers were dried over anhydrous $MgSO_4$, evaporated and purified by column chromatography on silica gel with hexane-ethyl acetate as the eluent to afford pure phenothiazenyl cyanoacrylamide **6a** as a dark red solid.

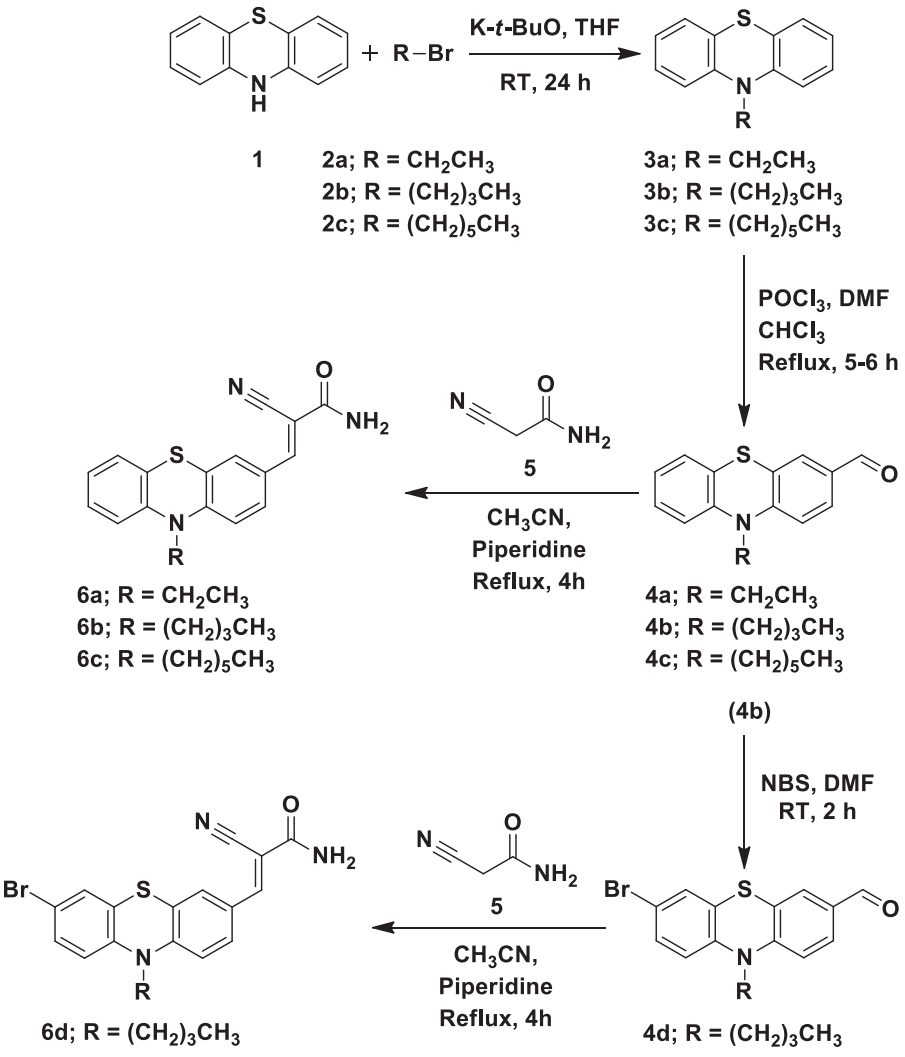

Scheme 1. Schematic representation for the synthesis of molecules **6a-d.**

Yield (86%); Melting point: 146–148 °C; FT-IR (KBr): ν_{max}/cm^{-1} 3408, 3153, 2879, 2206, 1691, 1565, 1471, 1440, 1367,1317, 1284, 1255, 1213, 1174, 1130, 1107, 956, 806, 742, 678, 655, 605, 534, 460; ^{1}H NMR (400 MHz, DMSO-d_6) δ 8.01 (1H, s), 7.77–7.82 (2H, m), 7.71 (1H, d, $J = 2.0$ Hz), 7.66 (1H, br s), 7.20 (1H, m),7.14 (2H, d, $J = 8.4$ Hz), 7.07 (1H, d, $J = 8$ Hz), 6.97 (1H, t, $J = 7.6$ Hz), 3.96 (2H, q), 1.30 (3H, t, $J = 6.8$ Hz); ^{13}C NMR (100 MHz, DMSO-d_6) 163.5, 149.5, 148.1, 142.9, 131.4, 128.6, 128.4, 127.6, 126.2, 123.9, 123.0, 121.8, 117.5, 116.3, 115.7, 103.1, 42.1, 12.8.

2.4. Synthesis of phenothiazenyl cyanoacrylamide **6b**

The phenothiazine carbaldehyde **4b** (0.56 g, 0.2 mmol), upon reaction with cyanoacetamide (0.17 g, 0.2 mmol) in acetonitrile furnished its corresponding phenothiazenyl cyanoacrylamide **6b** as a orange red solid. Yield (89%); Melting point: 125–127 °C; FT-IR (KBr): ν_{max}/cm^{-1} 3396, 3170, 2873, 2210, 1687, 1568, 1543, 1492, 1465, 1440, 1361, 1286, 1255, 1215, 1141, 1107, 956, 869, 800, 738, 663, 611, 540; ^{1}H NMR (400 MHz, $CDCl_3$) δ 8.13 (1H, s), 7.77 (1H, dd, $J = 8.8$ Hz, 1.6 Hz), 7.66 (1H, d, $J = 2$ Hz), 7.26 (1H, s), 7.18-6.85 (4H, m), 6.24 (1H, s), 5.65 (1H, s), 3.87 (2H, t, $J = 7.2$ Hz), 1.78 (2H, m), 1.44 (2H, m), 0.94 (3H, t, $J = 7.2$ Hz); ^{13}C NMR (100 MHz, $CDCl_3$) 162.8, 152.1, 149.5, 143.1, 131.2, 129.6, 127.6, 127.5, 125.7, 124.8, 123.6, 123.4, 117.7, 115.8, 114.9, 98.9, 47.6, 28.7, 20.0, 13.7.

2.5. Synthesis of phenothiazenyl cyanoacrylamide **6c**

The phenothiazine carbaldehyde **4c** (0.62 g, 0.2 mmol), upon reaction with cyanoacetamide (0.17 g, 0.2 mmol) in acetonitrile furnished its corresponding phenothiazenyl cyanoacrylamide **6c** as a dark red solid. Yield (87%); Melting point: 112–114 °C; FT-IR (KBr): ν_{max}/cm^{-1} 3400, 3165, 2960, 2933, 2872, 2210, 1687, 1568, 1494, 1465, 1442, 1361, 1313, 1288, 1251, 1213, 1143, 1107, 958, 879, 850, 806, 742, 663, 609, 536; ^{1}H NMR (400 MHz, $CDCl_3$) δ 8.12 (1H, s), 7.76 (1H, dd, $J = 8.8$ Hz, 1.6 Hz), 7.65 (1H, d, $J = 2.0$ Hz), 7.26 (1H, s), 7.18-6.84 (3H, m), 6.25 (1H, s), 5.72 (1H, s), 3.85 (2H, t, $J = 7.2$ Hz), 1.77 (2H, m), 1.42 (2H, m), 1.30 (4H, m), 0.90 (3H, br s); ^{13}C NMR (100 MHz, $CDCl_3$) 162.7, 152.2, 149.5, 143.1, 131.3, 129.6, 127.6, 127.5, 125.6, 124.8, 123.6, 123.3, 117.7, 115.8, 114.9, 98.9, 48.0, 31.3, 26.7, 26.5, 22.5, 13.9.

2.6. Synthesis of phenothiazenyl cyanoacrylamide **6d**

The phenothiazine carbaldehyde **4d** (0.72 g, 0.2 mmol), upon reaction with cyanoacetamide (0.17 g, 0.2 mmol) in acetonitrile furnished its corresponding phenothiazenyl cyanoacrylamide **6d** as a dark red solid. Yield (81%); Melting point: 130–132 °C; FT-IR (KBr): ν_{max}/cm^{-1} 3333, 3190, 2957, 2870, 2208, 1676, 1582, 1493, 1462, 1356, 1296, 1271, 1250, 1213, 1177, 1138, 1107, 955, 870, 804, 598, 542; ^{1}H NMR (400 MHz, $CDCl_3$) δ 8.13 (1H, s), 7.77(1H, dd, $J = 8.8$ Hz, 1.6 Hz), 7.63 (1H, d, $J = 2.0$ Hz), 7.20 (2H, m), 6.86 (1H, d, $J = 8.4$ Hz), 6.70 (1H, d, $J = 8.8$ Hz), 6.26 (1H, s), 5.75 (1H, s), 3.83 (2H, t, $J = 7.2$ Hz), 1.73 (2H, m), 1.43 (2H, m), 0.94 (3H, t, $J = 7.2$ Hz); ^{13}C NMR (100 MHz, $CDCl_3$) 162.8, 151.9, 149.0, 142.3, 131.3, 130.2, 129.7, 129.6, 126.0, 125.7, 124.1, 117.6, 116.9, 115.8, 115.1, 28.6, 20.0, 13.7.

2.7. Computational details

Computations of the target molecules **6a-d** have been performed with the Gaussian 09W packages [25]. The density functional theory calculations have been accomplished utilizing the hybrid functional B3LYP [26] with 6-311G(d,p) basis set. The theoretically computed frequency values at these levels contain

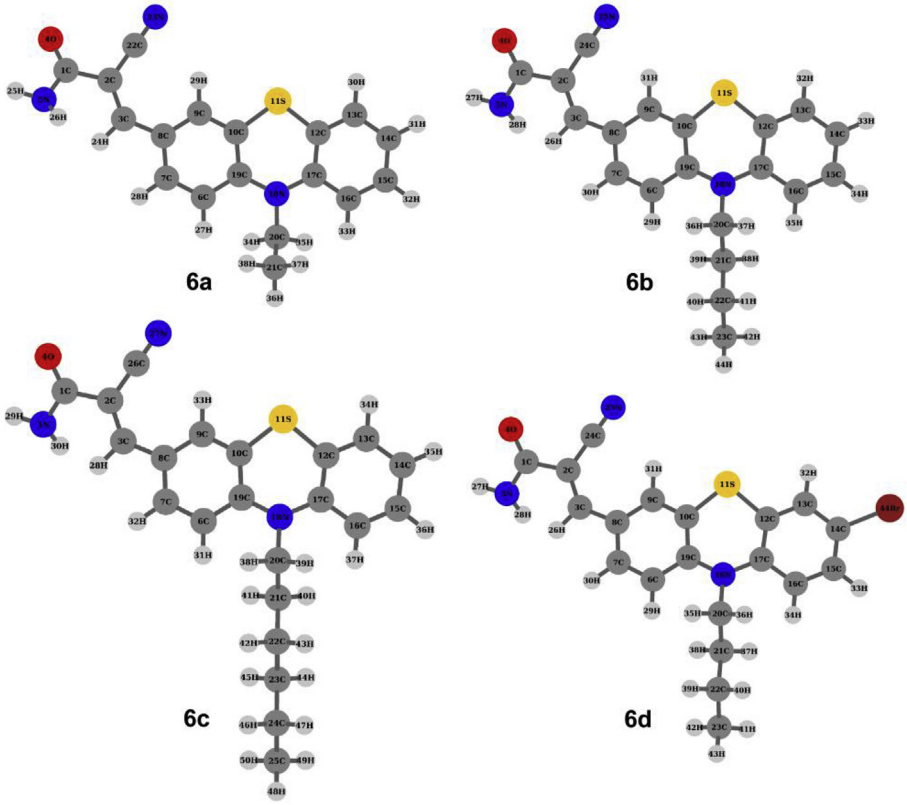

Fig. 1. Optimized structure of **6a-d.**

known systematic errors. To bring the theoretical frequencies in close proximity to the experimental values, the scaling factor value of 0.96 was used [27]. Frontier molecular orbitals (FMOs) and molecular electrostatic potential (MEP) are calculated to enlighten the possibility of the molecular interaction with other species around the space by sharing electronic charges.

2.8. DPPH scavenging activity

DPPH radical scavenging assay has been carried out using reported procedure [28] with slight modifications. The stock solution was prepared using DPPH (0.8 mg) in DMSO (25 mL). Various concentrations such as 10, 20, 30, 40, 50, 100 μg/ml of working solutions (compounds **6a-d**) were prepared to evaluate their radical scavenging activity. From the working solution, 1.5 ml of each compound was added with 1.5 ml of DPPH and kept for 30 min incubation under dark at room temperature. After incubation the absorbance was measured against the blank DPPH at 517 nm using UV−visible spectrophotometer. The percentage of DPPH radical scavenging activity was determined using the following equation (1),

$$\%\ \text{Scavenging} = 100 \times [(A_{control} - A_{sample})/A_{control}] \quad (1)$$

2.9. Cell lines and cell culture

Two human pancreatic cancer cells (AsPC1 and SW1990) were procured from the American Type Culture Collection, ATCC, USA. All cells were cultured in RPMI-1640 medium supplemented with 10% fetal bovine serum, 100 IU/mL of penicillin and 100 μg/mL of streptomycin (Sigma-Aldrich, St. Louis, MO, USA). All pancreatic cancer cells were maintained at an incubator at 37 °C in 5% CO_2, using the standard *in vitro* cell culture method established previously [29−33].

2.10. Cell viability assay

In order to evaluate the anti-tumor effects of the synthetic compounds, all compounds were reconstituted to 100 mM stock solution using dimethylsulfoxide, further diluted to sterile phosphate buffer saline to the highest effective concentration, 0.1 mM. The cells were treated based on the previously published cell viability assay [29,34]. Briefly, all cells were then seeded (1500 cells/well) in 384-well plates for 24 h before treated with compounds for 72 h. Cell viability was quantified using the CellTitre Glo Luminescent Cell Viability Assay (Promega, USA). The luminescence readings were recorded using SpectraMax M3 microplate reader (Molecular Devices Corporation, USA).

3. Results and discussion

3.1. Synthesis

The precursors, phenothiazine carbaldehydes **4a-c** have been synthesized *via* alkylation of 10*H*-phenothiazine with respective alkyl halides in the presence of potassium *tert*-butoxide in tetrahydrofuran at room temperature followed by Vilsmeier-Haack

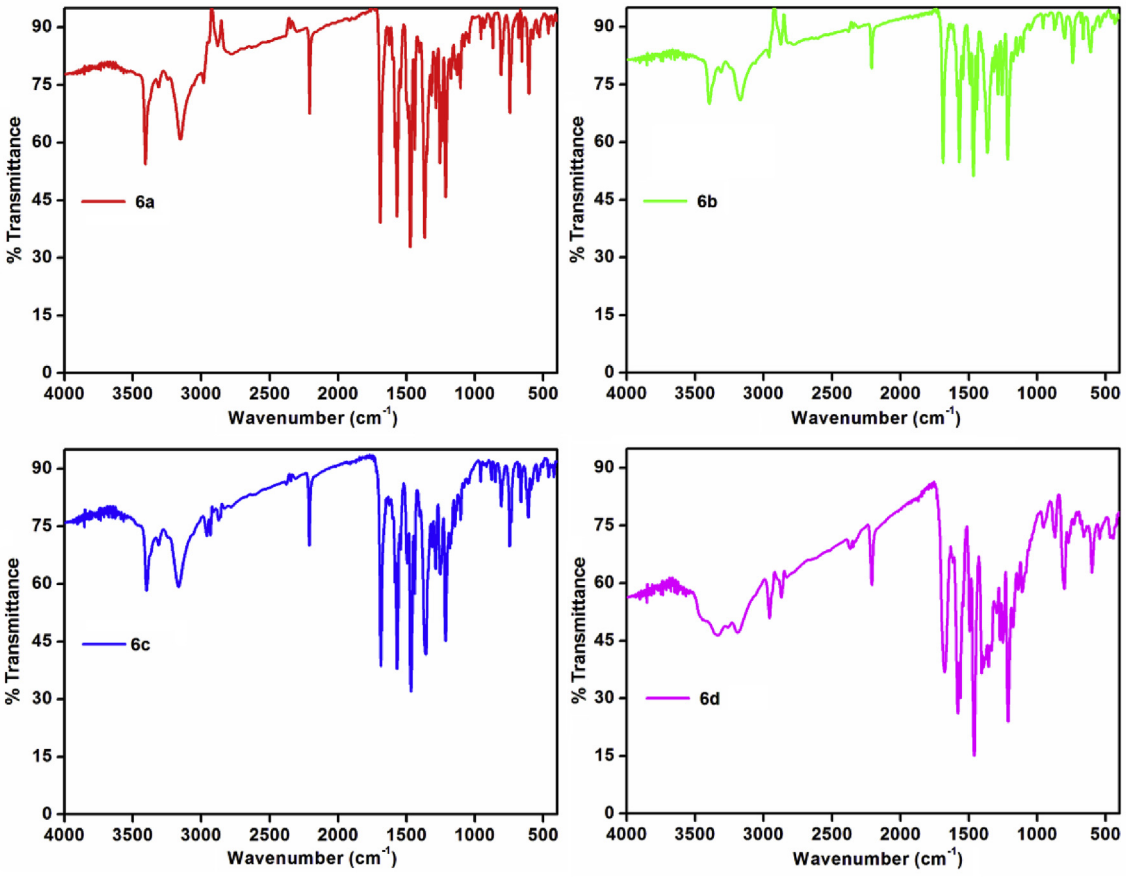

Fig. 2. Experimental FT-IR spectra of **6a-d.**

reaction of alkylphenothiazine with phosphoryl chloride in dimethylformamide at cooled to refluxed condition. On the other hand, the bromo substituted phenothiazine carbaldehyde **4d** has been synthesized by employing phenothiazine carbaldehyde **4b** with N-bromosuccinimide (NBS) at room temperature. Eventually, Knoevenagel condensation between respective phenothiazine carbaldehydes **4a-d** with cyanoacetamide (**5**) in the presence of piperidine in acetonitrile afforded the corresponding targets, phenothiazinyl cyanoacrylamides **6a-d** in good yields (Scheme 1). The chemical structures of the newly synthesized compounds **6a-d** have been established on the basis of analytical and spectral techniques.

3.2. Structural analysis

The synthesized target molecules **6a-d** have been optimized in ground state achieved by B3LYP/6-311G(d,p) method. The optimized molecular structure of the compounds **6a-d** is depicted in Fig. 1 and their selected bond lengths, bond angles and dihedral angles are presented in Table S1. Since the target molecules **6a-d** are new ones, it is obviously clear that the exact data resulted from experiments on the structural parameters of the same would not be accessible from the literature. Hence, it would not be feasible to compare the results of computation with the experiment. Consequently, the crystal information of strongly related molecules such as 10-ethyl-10*H*-phenothiazine-3-carbaldehyde [35] and 2-cyano-N-(furan-2-ylmethyl)-3-(3-nitrophenyl)propanamide [36] have been compared with that of the title molecules.

As can be seen from the figure, the orientation of donor and acceptor units (i.e. phenothiazine and acrylamide) are determined by dihedral angle for the compounds **6a-d** C2−C3−C8−C9/C7 by 4°/-4.7°/-4.6°/-5°and −176.2°/175.3°/175.6°/175.1° [35,36], respectively. Thus, the two units lie on the same plane which indicates strong electron delocalization occurs in the molecule. Further the phenothiazine ring flattening at S11 (99.4°/99.5°/99.4°/99.4°) and N18 (122.1°/122.2°/122.1°/122.3°) makes butterfly conformation which revealed that the flatted structure could devise the intramolecular charge transfer. The calculated bond parameters (*viz*., bond lengths and angles) associated with the phenothiazine and acrylamide part are expected in ideal range which is in good agreement with crystal data of the reported ones [35,36]. From the observation of computationally investigated molecules **6a-d**, a small deviation about 0.001 Å in bond length and 0.5−1.2° in bond angle as well as dihedral angle has been found for compounds **6a-d**.

3.3. FT-IR spectral analysis

The energy minima structures have been utilized for calculating vibrational frequencies of the synthesized compounds **6a-d** at B3LYP/6-311G(d,p) method and PED assignments have been achieved using VEDA program [37]. The compounds **6a-d** have 38/44/50/44 atoms, the molecules have normal modes of vibrations 108/126/144/126 and belong to C1 symmetry. All the 108/126/144/126 vibrational modes are equally disseminated as 40/46/52/46 stretching, 33/39/45/39 bending and 35/41/47/41 torsion vibrations in the computed spectrum. The experimental FT-IR of the compounds **6a-d** and their related computed ones under investigation are sketched in Fig. 2 and Fig. 3. The experimental and computed vibrational frequencies in addition to their relative intensities and plausible assignments of the compounds **6a-d** are furnished in

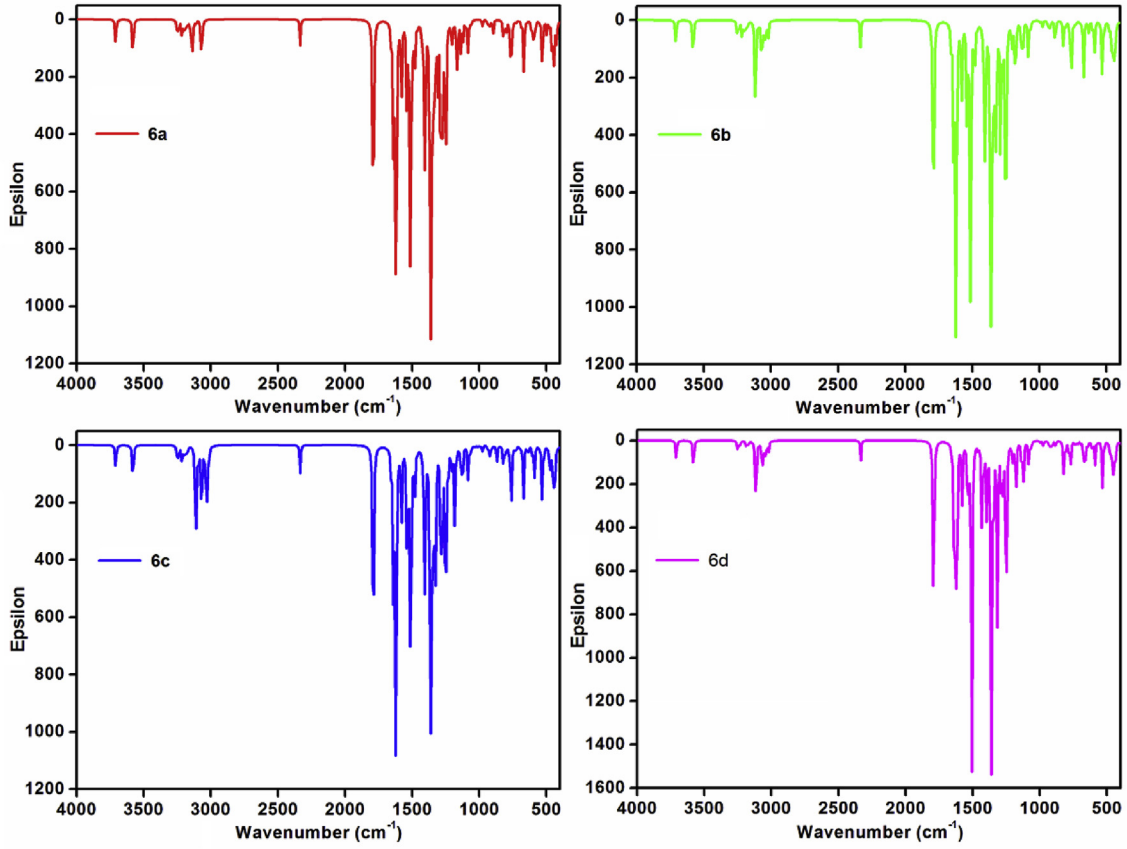

Fig. 3. Theoretical FT-IR spectra of **6a-d.**

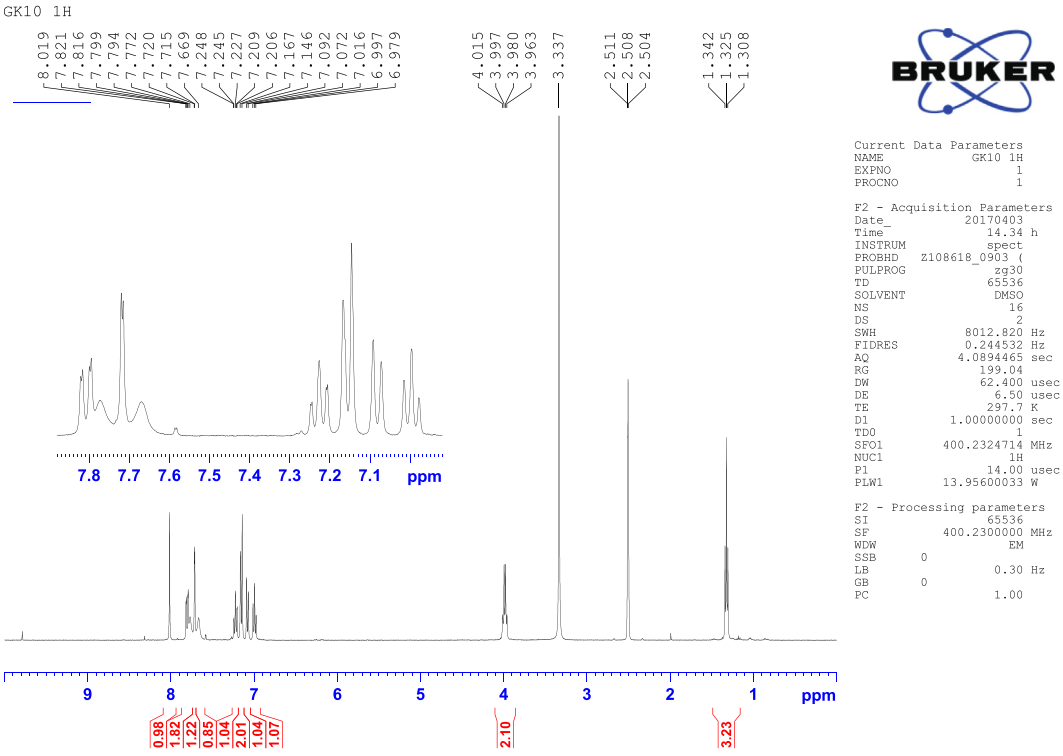

a

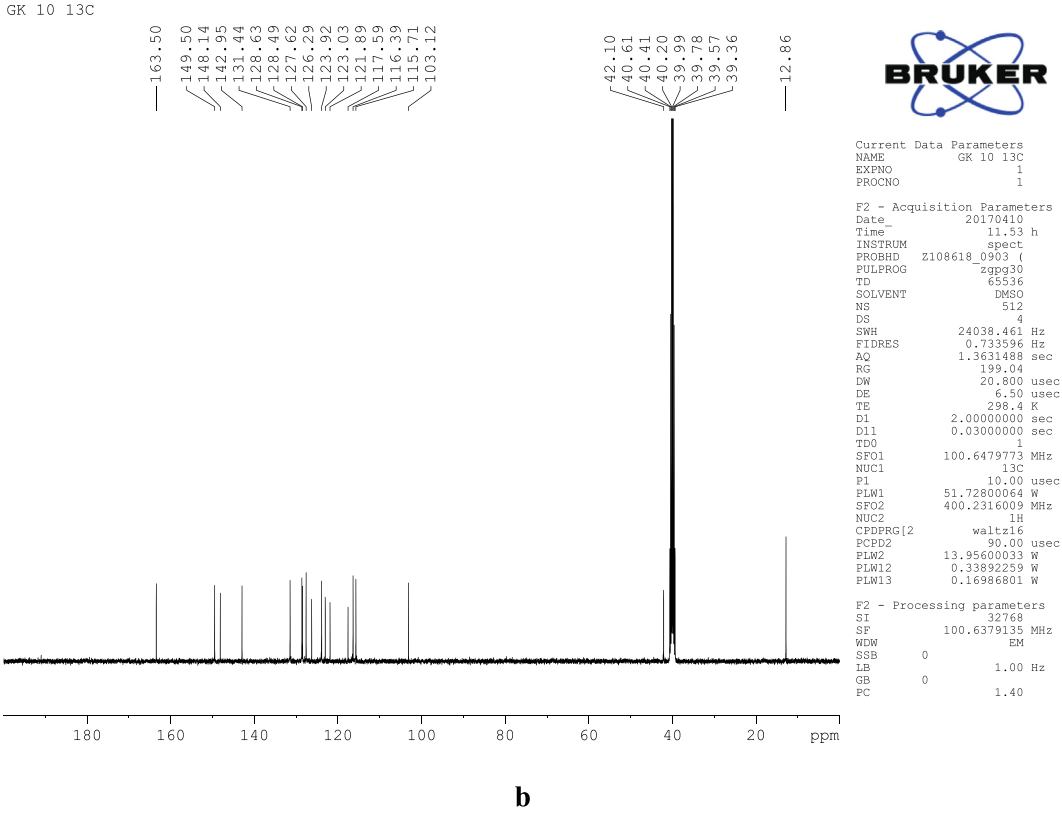

b

Fig. 4. (a) ^{1}H NMR spectrum of **6a**. (b) ^{13}C NMR spectrum of **6a.**

Tables S2–S5, respectively.

The unique stretching frequencies of aromatic $\nu_{C\text{-}H}$ generally emerged from the zone in the region 3100-3000 cm^{-1} [38]. In the experimental spectra of the compounds **6a-d**, an absorption bands exhibited in the region 3190-3153 cm^{-1} are owing to the aromatic $\nu_{C\text{-}H}$ stretching frequencies. These frequency values show good conformity with the theoretically computed ones, observed at 3121-3042 cm^{-1} in B3LYP calculations. The stretching frequencies of aliphatic $\nu_{C\text{-}H}$ usually arise at reasonably lesser frequencies than those present in the aromatic rings [39]. In the experimental spectra, the $\nu_{C\text{-}H}$ stretching vibrations of ethyl/butyl/hexyl side chains are resulted as medium and weak bands at 2960-2870 cm^{-1}. The calculated alkyl $\nu_{C\text{-}H}$ stretching vibrations are found in the region 3022-2890 cm^{-1}. Hence, the theoretical results are in accord with the experimental ones.

The symmetric and asymmetric stretching frequencies of aromatic and heteroaromatic ring systems are commonly arising in the area between 1625 and 1400 cm^{-1} [38]. In the FT-IR spectra of the compounds **6a-d**, the observed $\nu_{C\text{-}C}$ symmetric stretching frequencies appeared between 1581 and 1568 cm^{-1}. The computed frequencies predicted using B3LYP methods are 1593-1517 cm^{-1}, respectively. The carbon-carbon out-of-plane and in-plane bending vibrations of the compounds **6a-d** have been emerged at 1107-605 cm^{-1} while the corresponding computed ones are also appeared in a similar area and the results are tabulated in Table S2-**S5**, respectively.

Generally, the stretching vibrations of carbonyl are expected in the area from 1750 to 1650 cm^{-1} [38]. In the experimental case, the amidic carbonyl group $\nu_{C=O}$ present in the compounds **6a-d** gave an absorption bands at 1691-1676 cm^{-1}, while in the computational case, the carbonyl stretching bands arise at 1720-1718 cm^{-1}. These computed ones ($\nu_{C=O}$) are in harmony with their experimental counterparts.

In general, asymmetric and symmetric stretching frequencies of amino group of amide moiety resulted with strong intensity centred on 3500-3100 cm^{-1} [39]. In the compounds **6a-d**, a sharp band appeared in the region 3408-3332 cm^{-1} attributed to the presence of primary $\nu_{N\text{-}H}$ vibrations. The computationally calculated frequencies of these bands occurred at 3562-3439 cm^{-1} by DFT method which is coincide well with the experimental results.

The identification of C–N stretching vibrations is more complicated ones, since the mixing of several bands are possible in the region [40]. The sharp intense band resulted in the region 2210-2206 cm^{-1} is due to the characteristics of nitrile group present in the molecules. The DFT calculations gave the nitrile stretching frequencies at 2242-2241 cm^{-1}. The absorption modes are found in the region 1471-1361 cm^{-1} due to the C–N stretching of the compounds **6a-d**, while the corresponding computed frequencies lie at 1376-1296/1235-1222/1096-1085 cm^{-1}. The results reflect that the computed frequencies are aligned with their experimental ones.

The C–S group is less polar than carbonyl links and has considerably weaker bands in the infrared [40]. The C–S absorption band resulted in the FT-IR spectra of compounds **6a-d** at 673-663 cm^{-1} and the corresponding computed values are lie at 1029-1028/752-718/678-677/436-432 cm^{-1}.

The vibration frequencies belonging to CX groups (X = Cl, Br and I) usually occurred in the frequency range of 850-500 cm^{-1} [39]. In the experimental spectrum of compound **6d**, the absorption zones at 542 cm^{-1} is assigned to C–Br stretching vibrations of the molecule. The computed frequency of C–Br stretching band arise at 545 cm^{-1} by B3LYP/6-311G (d,p) coincided very well with the experimental value.

3.4. NMR spectral analysis

^{1}H NMR and ^{13}C NMR spectra of a representative molecule **6a** are depicted in Fig. 4a and b and the spectra of other molecules synthesized are given in Figs. S1–S3. The signals exposed in the

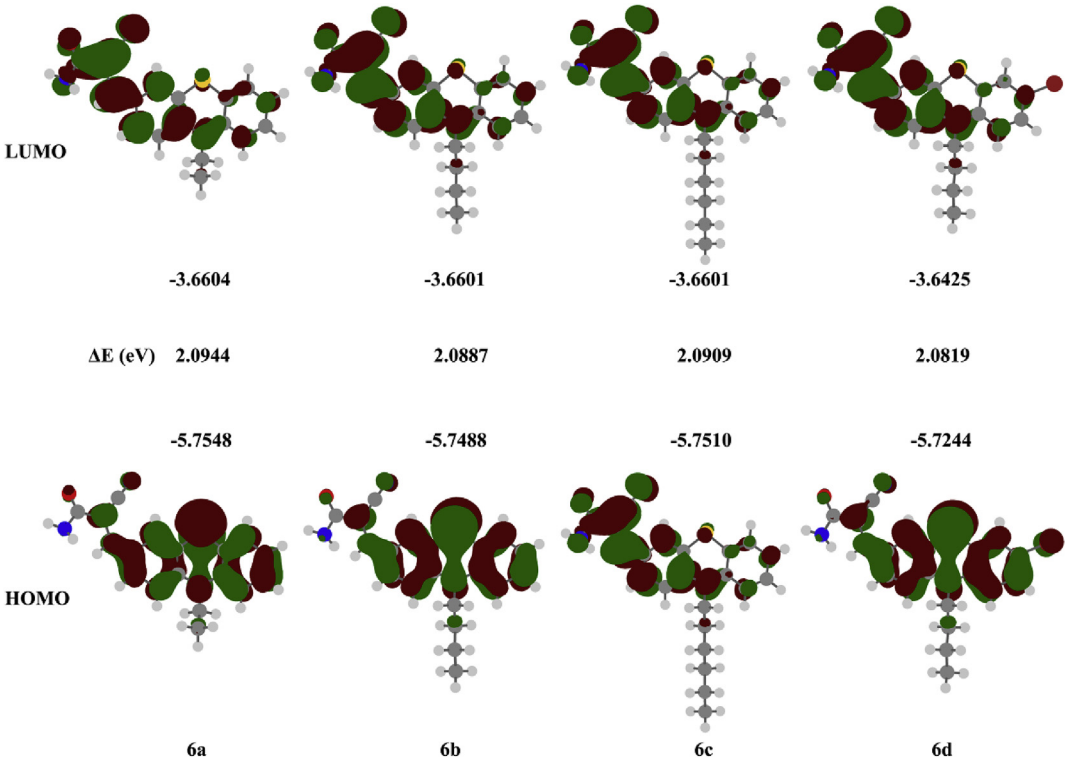

Fig. 5. 3D plots of frontier molecular orbitals of **6a-d.**

Table 1
Calculated frontier molecular orbital energies of **6a-d**.

	HOMO	LUMO	ΔE (eV)
6a	−5.7548	−3.6604	2.0944
6b	−5.7488	−3.6601	2.0887
6c	−5.7510	−3.6601	2.0909
6d	−5.7244	−3.6425	2.0819

shielded region of 0.88–4.01 ppm associated with triplets and multiplets correspond to the presence of alkyl groups present in the molecules. Two broad singlets resonated at 5.65–6.25 ppm with each one proton integral owing to the presence of amidic N–H protons. Multiplets observed in the region 6.97–7.82 ppm with seven/six protons integral are due to the presence of phenothiazine scaffold. A singlet resonated in the region 8.01–8.14 ppm corresponds to methine proton attached to the olefinic carbon. In the ^{13}C NMR, the signals resulted in the downfield region at 162.7–163.5 ppm are due to the presence of amidic C=O in the molecules. The aromatic/olefinic carbons are collectively resonated in downfield region at 103.1–152.2 ppm. Carbon signals for the alkyl side chain present in the molecule resonated in the range of 12.8–48.0 ppm.

3.5. Frontier molecular orbital analysis

Molecular orbitals of highest occupied and lowest unoccupied (MOs) are used to determine how the molecules interrelate with other species. Generally, compounds containing small energy gap exposed higher chemical reactivity, soft in nature, more polarized and low kinetic stability and, *vice versa* for compounds possess high energy gap [41]. The pattern of the HOMO and LUMO of the compounds **6a-d**, have been displayed in Fig. 5 and their energy values are summarized in Table 1. In the compound **6a**, the electron cloud of the HOMOs is highly populated in the phenothiazine ring and very tiny on the cyanoacrylamide motif. In contrast, the electron transition of the LUMOs is almost positioned in the cyanoacrylamide moiety and slightly on the phenothiazine motif. In the case of compounds **6b-d**, the HOMOs is delocalized over whole molecule except alkyl/amide group; however the LUMOs is mostly located on cyanoacrylamide group. Thus, the electron distribution profile of compounds **6a-d** clearly states that the electron flow could be efficiently transferred from phenothiazine ring to cyanoacrylamide unit.

The computed HOMO and LUMO energy of the compound **6a** is −5.7548 eV and −3.6604 eV, the resulting band gap energy (ΔE) of the compound **6a** is 2.0944 eV. Similarly, in the compounds **6b-d**, the energy have been calculated for HOMOs as −5.7488 eV, −5.7510 eV and −5.7244 eV while for LUMOs as −3.6601 eV, −3.6601 eV and −3.6425 eV, which result the band gap energy of 2.0887 eV, 2.0909 eV and 2.0819 eV.

3.6. Molecular electrostatic potential analysis

Molecular electrostatic potential (MEP) is a powerful tool to identify the electrophilic and nucleophilic reactive sites of molecule and it is very valuable in research of molecular structure with its relationship of physiochemical properties. A model of electrostatic potential of the compounds **6a-d**, computed at the 0.002 a.u isodensity surface is furnished in Fig. 6. From the MEP image of the

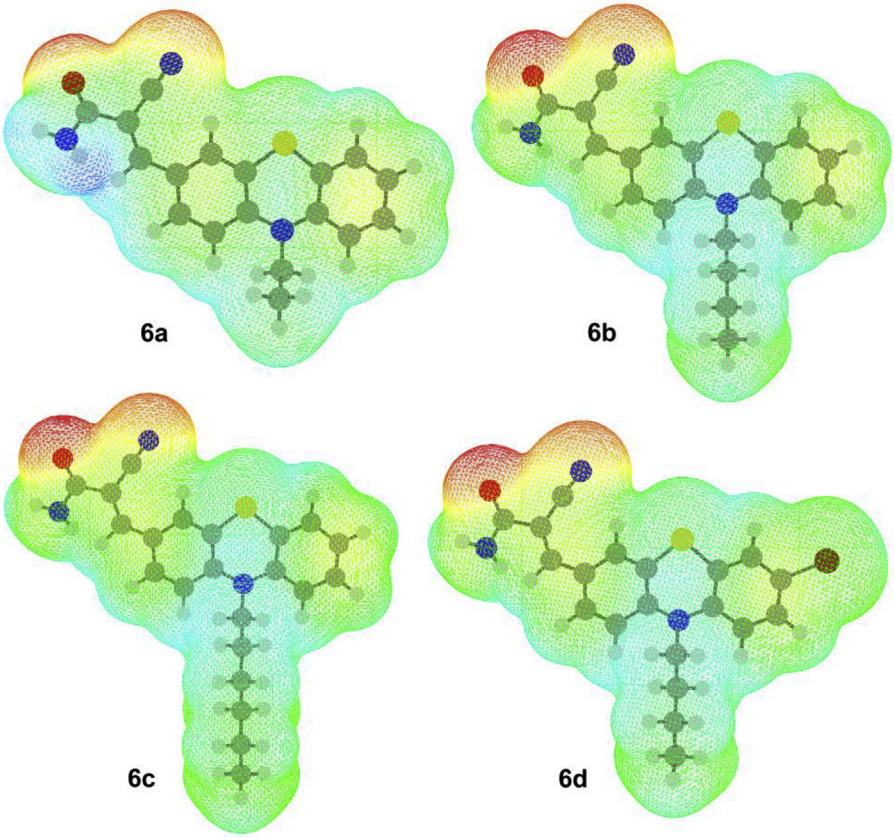

Fig. 6. Molecular electrostatic potential surfaces of **6a-d.**

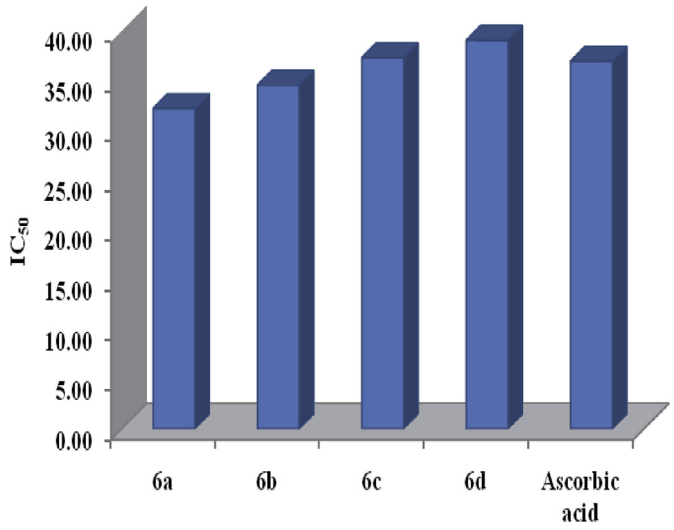

Fig. 7. Antioxidant activity of molecules **6a-d.**

compound **6a**, one can observe that the negative potential are characterized on most electron abundant nitrile and amide carbonyl part. The positive region is typically distributed on the amide NH_2. Similarly, the MEP image of the compounds **6b-d**, the negative potential is polarized over the nitrile and amide carbonyl unit. However, the light yellow region spread over the phenothiazine ring while the green region covers the whole molecular surface. Thus, these locations provide the information about the area from where the compound can be devised the intermolecular interactions. Therefore, the most feasible reactive sites of the compounds **6a-d** could be involved as an electrophilic reactive site at C1=O4 and C22≡N23.

3.7. DPPH radical scavenging activity

The *in vitro* radical scavenging activity of the synthesized compounds **6a-d** has been evaluated using 2,2-diphenyl-1-picrylhydrazyl (DPPH) method and their results are provided in Fig. 7 and Table 2. The data of radical scavenging activity reveals that the synthesized compounds **6a-d** exhibited moderate to excellent activity against the reference drug ascorbic acid. Interestingly, the molecule with butyl substitution on the nitrogen of the phenothiazine core along with bromo substituent on the sixth position of the same (**6d**) has found to be better one when compared to ascorbic acid, the standard antioxidant (IC_{50} 39.07 μM) while the molecule possessing hexyl substitution on the nitrogen of the phenothiazine structural unit (i.e., **6c**) exhibited slightly lower activity (IC_{50} value 37.32 μM) when compared to the standard. Besides, the privileged molecules **6a** and **6b** exposed comparatively lower radical scavenging activity along with IC_{50} value of 32.08 and 34.55 μM, respectively.

3.8. Anticancer activity

The *in vitro* anticancer activity of the synthesized molecules **6a-d** have been evaluated against two human pancreatic cancer cell lines *viz*., AsPC1 and SW1990. The results of cytotoxic effect of the compounds **6a-d** have been presented in Table 3. All the tested compounds **6a-d** demonstrated moderate to good *in vitro* anticancer activities towards the tested pancreatic cancer cell lines. Among them, the compound **6c** which holds hexyl group on the nitrogen of the phenothiazine motif exhibited the highest anticancer activity against SW1990 while the compounds **6b** and **6d** displayed good anticancer activity against SW1990. Besides, the molecule **6a** showed moderate anticancer activity against SW1990. On the other hand, it was also observed that the compounds **6b, 6c** and **6d** exhibited significant anticancer activity against AsPC1 pancreatic cancer cell line while the compound **6a** was found to be moderately active against AsPC1 cancer cell line. It could be inferred that the anticancer activity of compounds increases with the increase of alkyl chain length attached at the nitrogen atom of the phenothiazine ring. Based on the alkyl substitution, the anticancer activity decreases in the order of ethyl < bromo substituted butyl < butyl < hexyl substituent.

4. Conclusion

Synthesis of the newly designed phenothiazine based cyanoacrylamides **6a-d** was achieved from commercially available phenothiazine using multistep synthetic approach. The structures of the target compounds (**6a-d**) were established by physical and spectroscopic methods *viz*, FT-IR, ^{1}H NMR and ^{13}C NMR. Computational studies for the target molecules **6a-d** have been performed to realize the physiochemical properties. DPPH method has been exploited to study the in *vitro* radical scavenging activity of the privileged molecules **6a-d**. Of those, the **6b** and **6c** exhibited high radical scavenging activity towards DPPH. Further, the synthesized new compounds have been subjected to *in vitro* anticancer evaluation against a couple of pancreatic tumor cells AsPC1 and SW1990. Among them, the molecule **6c** has been identified as the most potent one against both the tumor cells *viz*., AsPC1 and SW1990. The results imply that these new compounds could serve as valuable intermediates for the construction of efficient radical scavenger/anticancer agents. In order to improve the activities further, structural diversification of this category of molecules is under progress.

Table 3
In vitro anticancer activity of **6a-d**.

S.No.	Compound	Cell viability	
		SW1990	AsPC1
1	6a	44.10	46.23
2	6b	20.70	30.72
3	6c	13.30	25.32
4	6d	22.63	30.44

Table 2
Antioxidant activity of **6a-d**.

S.No.	Compound	100 μM	50 μM	40 μM	30 μM	20 μM	10 μM	IC_{50} μM
1	6a	69.49	61.77	59.45	56.37	49.61	43.43	32.21
2	6b	82.23	77.41	71.62	65.63	57.91	54.82	34.56
3	6c	80.30	74.51	68.91	60.42	56.75	52.12	37.32
4	6d	76.44	68.53	61.77	57.14	51.54	45.94	39.08
5	Ascorbic acid	88.22	82.62	78.18	73.35	68.14	65.05	36.97

Acknowledgements

Financial assistance provided by the Indian Council of Medical Research, New Delhi (No.58/16/2013BMS) and Kalasalingam Academy of Research and Education (PDF to KG) is gratefully acknowledged.

Appendix A. Supplementary data

Supplementary data to this article can be found online at https://doi.org/10.1016/j.molstruc.2019.127037.

References

[1] Cancer, world health organization: WHO. http://who.int/cancer/en.
[2] Cancer, national cancer institute: NCI. http://www.cancer.gov.
[3] M. Iwata, L. Hirose, H. Kohara, J. Liao, R. Sawada, S. Akiyoshi, K. Tani, Y. Yamanishi, J. Med. Chem. 61 (2018) 9583–9595.
[4] B. Kuhn, P. Mohr, M. Stahl, J. Med. Chem. 53 (2010) 2601–2611.
[5] A. Alex, D.S. Millan, M. Perez, F. Wakenhut, G.A. Whitlock, Med. Chem. Commun. 2 (2011) 669–674.
[6] E. Vitaku, D.T. Smith, J.T. Njardarson, J. Med. Chem. 57 (2014) 10257–10274.
[7] https://en.wikipedia.org/wiki/Chlorpromazine.
[8] https://en.wikipedia.org/wiki/Trifluoperazine. https://en.wikipedia.org/wiki/Thioridazine. https://en.wikipedia.org/wiki/Promethazine. https://de.wikipedia.org/wiki/4-Azaphenothiazin.
[9] K. Pluta, M. Jelen, B. Morak-Mlodawska, M. Zimecki, J. Artym, M. Kocieba, E. Zaczynska, Eur. J. Med. Chem. 138 (2017) 774–806.
[10] K. Pluta, B. Morak-Mlodawska, M. Jelen, Eur. J. Med. Chem. 46 (2011) 3179–3189.
[11] G. Spengler, A. Csonka, J. Molnar, L. Amaral, Anticancer Res. 36 (2016) 5701–5706.
[12] S. Wang, B. Zhang, W. Wang, G. Feng, D. Yuan, X. Zhang, Chem. Eur J. 24 (2018) 8157–8166.
[13] B.-H. Chiou, Y.-T. Tsai, C.M. Wang, Langmuir 30 (2014) 1550–1556.
[14] A.N. Matralis, A.P. Kourounakis, J. Med. Chem. 57 (2014) 2568–2581.
[15] M.-J. Park, J. Lee, I.H. Jung, J.-H. Park, D.-H. Hwang, H.-K. Shim, Macromolecules 41 (2008) 9643–9649.
[16] S. Kumar, M. Singh, J.-H. Jou, S. Ghosh, J. Mater. Chem. C 4 (2016) 6769–6777.
[17] S. Feng, Q.-S. Li, T.A. Niehaus, Z.-S. Li, Org. Electron. 42 (2017) 234–243.
[18] K. Stalindurai, A. Karuppasamy, J.-D. Peng, K.-C. Ho, A. Tamilselvan, Tetrahedron 73 (2017) 278–289.
[19] a) J.S. Miller, J.L. Manson, Acc. Chem. Res. 34 (2001) 563–570;
b) H. He, P. Tran, H. Yin, H. Smith, Y. Batard, L. Wang, H. Einolf, H. Gu, J.B. Mangold, V. Fischer, D. Howard, Drug Metab. Dispos. 37 (2009) 536–544.
[20] F.F. Fleming, Nat. Prod. Rep. 16 (1999) 597–606.
[21] F.F. Fleming, L. Yao, P.C. Ravikumar, L. Funk, B.C. Shook, J. Med. Chem. 53 (2010) 7902–7917.
[22] C. Jin, X. Wu, Y. Zhang, Food Res. Int. 51 (2013) 611–620.
[23] J.-Q. Yang, B.-A. Song, P.S. Bhadury, Z. Chen, S. Yang, X.-J. Cai, D.-Y. Hu, W. Xue, J. Agric. Food Chem. 58 (2010) 2730–2735.
[24] K.D. Upadhyay, N.M. Dodia, R.C. Khunt, R.S. Chaniara, A.K. Shah, ACS Med. Chem. Lett. 9 (2018) 283–288.
[25] M.J. Frisch, Gaussian 09, Revision E.01, Gaussian, Inc., Wallingford CT, 2009.
[26] a) C. Lee, W. Yang, R.G. Parr, Phys. Rev. B 37 (1988) 785–789;
b) A.D. Becke, J. Chem. Phys. 98 (1993) 5648–5652.
[27] G. Rauhut, P. Pulay, J. Phys. Chem. 99 (1995) 3093–3100.
[28] K. Thaipong, U. Boonprakob, K. Crosby, L. Cisneros-Zevallos, D.H. Byrne, J. Food Compost, Analyst 19 (2006) 669–675.
[29] J.L. Er, P.N. Goh, C.Y. Lee, Y.J. Tan, L.-W. Hii, C.W. Mai, F.F.-L. Chung, C.-O. Leong, Apoptosis 23 (2018) 343–355.
[30] F.F.-L. Chung, P.F.T.M. Tan, V.J. Raja, B.-S. Tan, K.-H. Lim, T.-S. Kam, L.-W. Hii, S.H. Tan, S.-J. See, Y.-F. Tan, L.-Z. Wong, W.K. Yam, C.W. Mai, T.D. Bradshaw, C.-O. Leong, Sci. Rep. 7 (2017) 1–13.
[31] K.Y. Yeong, S.C. Tan, C.-W. Mai, C.-O. Leong, F.F.-L. Chung, Y.K. Lee, C.F. Chee, N.A. Rahman, Chem. Biol. Drug Des. 91 (2018) 213–219.
[32] C.-W. Mai, Y.-B. Kang, V.D. Nadarajah, A.S. Hamzah, M.R. Pichika, Phytother Res. 32 (2018) 1108–1118.
[33] C.W. Mai, K.S.I. Yap, M.T. Kho, N.H. Ismail, K. Yusoff, K. Shaari, S.Y. Chin, E.S.H. Lim, Front. Pharmacol. 7 (2016) 1–11.
[34] H.-C. Soo, F.F.-L. Chung, K.-H. Lim, V.A. Yap, T.D. Bradshaw, L.-W. Hii, S.-H. Tan, S.-J. See, Y.-F. Tan, C.-O. Leong, C.-W. Mai, PLoS One 12 (2017) 1–20.
[35] D.-H. Yu, J.-Q. Wang, L. Konga, Z.-D. Liu, Acta Crystallogr. E67 (2011) o3344.
[36] S. Subhadramma, B.P. Siddaraju, N. Chandra, J. Saravanan, D. Gayathri, Acta Crystallogr. E71 (2015) o568–o569.
[37] M.H. Jamroz, Spectrochim. Acta, Part A 114 (2013) 220–230.
[38] B.H. Stuart, Infrared Spectroscopy: Fundamentals and Applications, John Wiley and Sons, Chichester, UK, 2004.
[39] R.G. Snyder, H.L. Strauss, C.A. Elliger, C-H stretching modes and the structure of n-alkyl chains. 1. Long, disordered chains, J. Phys. Chem. 86 (1982) 5145–5150.
[40] G. Socrates, Infrared and Raman Characteristic Group Frequencies, Tables and Charts, third ed., Wiley, Chichester, 2001.
[41] I. Fleming, Frontier Orbitals and Organic Chemical Reactions, Wiley-Blackwell, New York, 1976.